Surface preparation of porous Si-graphene nanocomposites for heteroepitaxy

Mourad Jellite, Maxime Darnon, Roxana Arvinte, Mohammad Reza Aziziyan, Denis Machon, Abderraouf Boucherif, Richard Arès

Surface preparation of porous Si – graphene nanocomposites for heteroepitaxy

Mourad Jellite, Maxime Darnon, Roxana Arvinte, Mohammad Reza Aziziyan, Denis Machon, Abderraouf Boucherif, and Richard Arès*

Institut Interdisciplinaire d'Innovation Technologique (3IT), Université de Sherbrooke, 3000 boul. de l'Université, Sherbrooke, Québec J1K 0A5, Canada. and

Laboratoire Nanotechnologies Nanosystèmes (LN2) - CNRS UMI-3463, Université de Sherbrooke, 3000 Boulevard Université, Sherbrooke, J1K OA5, Québec, Canada.

(Dated: August 27, 2020)

Abstract

We have investigated the fabrication process of an alternative approach for a direct integration of epitaxial structures onto a foreign substrate. Our approach is based on the synthesis of a nanocomposite made of graphene-like carbon and porous silicon (GPSi). The nanocomposite was produced by anodization etching of a silicon substrate, followed by a thermal carbonization step. The main study focused on the preparation of the nanocomposite surface for subsequent epitaxial deposition. While the nanocomposite must retain its carbon content for thermal stability at epitaxial temperatures, the surface must be stripped of its residual carbon to expose the silicon crystal and support the layer nucleation. Our results show that the porous silicon (PSi) substrate, carbonized at 750°C and subjected to an O_2 plasma treatment of 20W during 12s, presented a carbon-free surface, while the bulk porous structure retained its carbon coating. Subsequent growth of a crystalline GaAs thin film demonstrated the substrate ability to support epitaxy.

* richard.ares@usherbrooke.ca

I. INTRODUCTION

The evolution of heteroepitaxial growth of semiconductors has made tremendous advances in many fields such as energy harvesting, communication, imaging and sensing systems, thanks to the nanoscale controlled material deposition techniques[**?**]. For example, monolithic integration of different components fabricated with various semiconductors, into one platform, typically silicon (Si), attracted the attention of many research groups because of the maturity of technology and lower cost of the substrate. However, there are still some major challenges that prevent such integration.

It is well known in the literature that the difference in lattice parameters between the epitaxial layer and the substrate prevents defect-free heteroepitaxy[**?**]. Basically, as epitaxy proceeds, the layer is strained, but it remains coherent with the substrate as long as its thickness is below a certain threshold, known as critical thickness[**?**]. Once the layer thickness reaches this critical value, segments of misfit dislocations are generated to relax the excess strain imposed by the lattice mismatch. These misfit dislocations are coupled to threading components that emerge at the layer surface, crossing the active region and creating non-radiative defects that are detrimental to the device performances[**?**].

Since the 80s, many approaches such as thick metamorphic buffer layers, wafers bonding, epitaxial liftoff, layer transfer and freestanding membranes have been developed to attempt at reducing dislocation propagation[**? ? ?**]. Substrate modification through surface patterning has also been widely studied and seems to be seen as a promising method that can pave the way for the fabrication of low-dimension devices[**?**]. However, these approaches are all suffering from some level of complexity and difficulty in their implementation, preventing most of them from broad industrial deployment. In its quest for the "ultimate" substrate for heteroepitaxy, our group has recently developed a novel compliant substrate based on graphene-porous Si nanocomposites (GPSi)[**?**]. The GPSi substrates have remarkable elastic properties and thermal stability, which makes a good candidate for strain accommodation during epitaxial growth[**? ?**]. Nevertheless, an efficient preparation step prior to epitaxial growth is required in order to produce clean, crystalline and carbon-free surface, while maintaining a thermally stable nanocomposite structure.

In this paper, we discuss a specific preparation scheme of the GPSi substrate surface for subsequent growth of Gallium Arsenide (GaAs) thin films as shown in Fig. 1. The process flow begun with the fabrication of GPSi substrate having C-coating all over the surface, followed by

Figure 1: Schematic representation of carbon-free surface preparation of GPSi substrate for epitaxial growth showing the main steps: (1) surface cleaning, where oxygen plasma etch carbon atoms from the topmost surface of GPSi and (2) epitaxial growth of thin film on the carbon-free surface of O_2-GPSi substrate.

the surface cleaning step (1) where oxygen plasma etch C-coating from the topmost surface of GPSi producing O2-GPSi substrate and ending with the epitaxial growth step (2) of GaAs epilayer on the top of O2-GPSi substrate.

II. EXPERIMENTAL

A. Substrate Modification

The substrate modification starts with the porosification of a p-type Si (001) substrate with a resistivity ranging from 0.01 to 0.02 Ωcm. The porosification step was carried out in a Kymosis O-ring anodization cell and a hydrofluoric acid (49%) and ethanol (1:1) volume ratio electrolyte solution. The porous Si (PSi) layer was formed by using a current density of 100 mA cm^{-2} (*i.e.* , by applying an alternating current), which provides a layer porosity of $\sim$ 55% and an average pore diameter of $\sim$ 10 nm. Further on, the obtained PSi is subjected to a carbonization step to form the GPSi nanocomposite structure. The carbonization process was carried out in a quartz tube furnace under a mixed gas atmosphere composed of argon (Ar), hydrogen (H_2) and acetylene (C_2H_2), with a flow rate of 450, 100 and 5 sccm, respectively. The deposition temperature and duration were fixed at 750°C and 10min for all samples. In order to obtain the clean, crystalline and carbon-free surface required for heteroepitaxy, the GPSi substrates were exposed to oxygen (O_2) plasma process. The O_2 plasma etching was performed in a barrel type chamber, under a pressure of 300mTorr and a radio frequency (RF) power of 20W. The exposure time to O_2 plasma was varied in the range of 12-300s.

B. Epitaxial Growth

The epitaxial growth of GaAs films was carried out in a VG SemiconVG90H Chemical Beam Epitaxy (CBE) reactor under an operating pressure of 2.7x10^{-4} mTorr. Three porous structures PSi, GPSi and O_2 treated GPSi (O_2-GPSi) were used as substrates. Triethylgallium (TEGa) and cracked arsine (AsH3) were used as group III and V precursor sources, respectively. Before each epitaxial growth, the substrates were rinsed under diluted HF solution to remove the native oxide, blown dry with nitrogen and introduced into the CBE growth chamber. Afterwards, all the substrates were preannealed at $\sim$ 650°C for 10 min inside the CBE reactor. Then, the growth temperature was set down to $\sim$ 565°C and was monitored during the deposition process by an in-situ absorption band-edge spectroscopy (ABES) system. The growth rate was determined at $\sim$ 0.25nm s^{-1}.

C. Materials Characterization

The carbon presence and crystalline structure of the GPSi nanocomposite were evaluated by Raman spectroscopy with a 532nm wavelength green laser source. Zeiss Leo 1530 VP scanning electron microscope (SEM) was used to characterize the structural morphologies and thicknesses of the porous-based substrates and GaAs thin films. Surface roughness of porous-based substrates and GaAs thin films were determined by an atomic force microscope (AFM) using a Veeco Dimension 3100 workstation. X-ray diffraction (HR-XRD) measurements using a Philips X'Pert diffractometer were performed to analyze the crystalline structure of the GaAs films grown on the three porous-based PSi, GPSi and O2-GPSi substrates.

III. RESULTS AND DISCUSSION

A. Surface cleaning

Fig. 2 shows the Raman spectra of PSi, GPSi and O_2-GPSi substrates. The analyzed O_2-GPSi substrate was processed with a 20W power O_2 plasma etching during 12s. For PSi substrate, the Raman spectrum shows a well-defined first order Si-related peak situated at $\sim 519\text{cm}^{-1}$. The peaks located at $\sim 300\text{cm}^{-1}$ and $\sim 950\text{cm}^{-1}$ are attributed to second-order modes of Si[**?**]. As expected the Raman spectrum of GPSi substrate, presents in addition to Si modes, the signatures of two first-order C-related peaks at $\sim 1350\text{cm}^{-1}$ and $\sim 1600\text{cm}^{-1}$, respectively, identified as D and G bands of carbon. The D-band is related to defects within the material linked to carbon (C)[**? ?**], while G-band is associated to carbon sp2 hybridization (*i.e.* in plane C-C stretching)[**? ?**]. Two other less intense peaks are noticeable on the spectrum at $\sim 2700\text{cm}^{-1}$ and $\sim 3000\text{cm}^{-1}$, and are associated to 2D and S3 graphene-related signal[**? ?**]. The I_D/I_G ratio was determined at 1.07, which suggests a high density of defects in the GPSi substrate. The defects seem similar with the ones found in three-dimensional graphene layers "3D nanographene"[**?**]. On the O_2-GPSi substrate, as in the case of GPSi substrate, first and second order Si-Si peaks and carbon-related peaks are displayed at similar positions as the ones described above. Moreover, we noticed a diminution of the D and G peak intensity, which can be explained by the etching of carbon at the nanocomposite surface. It is important to point out that the samples showed a uniform Raman spectrum over the surface of the measured samples (*see Fig. S1, supporting information file*).

To further investigate the effect of O_2 plasma etching on the GPSi substrate, samples with

various plasma exposures time, while the O_2 plasma power was kept constant at 20W were characterized. The exposure times used for the study were 12s, 42s, 60s and 300s, respectively. The inset A of Fig. 2 display the evolution of the area of the D and G peaks region (A_{D+G}) of O_2-GPSi samples normalized by the A_{D+G} peak area of GPSi substrate as a function of O_2 plasma exposure time. We notice that the A_{D+G} ratio decreases with the increase in O_2 plasma exposure time. This behavior is similar to what is observed in porous low-k dielectrics (used for CMOS interconnects) exposed to plasma processes[**? ? ?**]. It is known that porous low-k dielectric materials exposed to an O_2-based plasma show a bilayer structure with a fully carbon-depleted layer on a hardly modified porous low-k [**? ? ?**]. The thickness of the C-depleted layer increases with the exposure time to O_2 plasma . Kunnen et al.[**?**] showed that the carbon depletion is first limited by oxygen radical diffusion, and then by a competition between oxygen diffusion and recombination with adsorbed oxygen inside the porous structure.

In our conditions, the evolution of the A_{D+G} ratio plotted in the insert A of Fig. 2 includes both the evolution of the thickness of the carbon-depleted layer as a function of the plasma exposure duration and the non-linear effect of the Raman spectroscopy response due to Beer-Lambert's law, hence a direct fit is therefore not straightforward. Nonetheless, our data indicate a very fast decrease of the carbon content (30% in 12s) followed by a slower decay, which is compatible with the diffusion/recombination mechanism, as proposed by Kunnen et al.[**?**] for porous low-k exposed to plasma processes. At short exposure time ($\leq$12s), carbon removal is dominated by direct reaction with oxygen radicals. For a longer time (>12s), the removal is limited by the diffusion of oxygen radicals inside the pores that competes with their recombination into O_2 molecules[**?**]. Based on the exposed mechanisms, the exposure time should be as short as possible for a stripping of carbon, exclusively from the top surface of GPSi substrates by oxygen radicals. A slightly longer exposure time would allow the diffusion of oxygen radicals inside the porous material that will strip the carbon within the pores. To remain in a reproducible and controllable regime for our plasma chamber, we used the smallest process time of 12s in the rest of this paper.

In order to estimate the thickness of the carbon-depleted layer, we performed complementary experiments with various incoming GPSi layer thicknesses. The inset B of Fig. 2 shows the A_{D+G} as a function of GPSi's porous layer thickness. The corresponding Raman spectra and SEM images are presented in *Fig. S2, supporting information file*. The thickness of the GPSi layer was varied from 125nm up to 573nm. The O_2 plasma power and exposure time were kept constant at 20W and 12s, respectively. We can observe that increasing the thickness of the GPSi results

Figure 2: Raman spectra of PSi , GPSi and O_2-GPSi substrates. O_2-GPSi was processed with a 20W plasma for up to 12s. Inset (A) illustrates the evolution of normalized D and G peak area (A_{D+G}) ratio as a function of O_2 plasma exposure time. Inset (B) shows the A_{D+G} ratio as function of GPSi layer thickness.

in an increase of the A_{D+G} ratio from Raman spectra. Giving the fact that GPSi nanocomposite is complex material, we developed a simple model to estimate roughly to the thickness of the carbon-depleted layer from the experimental data of inset B in Fig. 2. In this model, we neglect both transmittance and reflectance of the green laser light by GPSi nanocomposite and we consider only Raman scattering (S) and absorbance (A), implying that $S+A \approx 1$, so that we can correlate the Raman scattering to an absorbance of the nanocomposite, by using the Beer-Lambert's law as follows:

$$S(t) \approx C.(1-A(t)) \approx C.[1-exp(-\alpha(t-d))] \quad (1)$$

Where C, α, t and d are the proportionality factor, the absorption coefficient of GPSi (at $\lambda =$

532nm), the thickness of GPSi layer and the thickness of the carbon-depleted layer, respectively. In addition, we consider that the carbon-depleted layer has a small absorbance and does not alter the Raman scattering of the main GPSi layer. So, we neglected its contribution term ($exp(-\alpha.d)$) in the beer-Lambert's equation (1). Also, knowing that the underlying bulk Si is transparent in the wavelength range of D and G graphene's peaks, so does not interfere with the Raman scattering of the main GPSi layer.

Based on all these assumptions, our model provides a carbon-depleted layer thickness of $d =$ 64nm, corresponding to the intercept of the fit with the thickness axis. The best fit parameters $C = 0.88$ and $\alpha = 1x10^5 \text{cm}^{-1}$, seem to be reasonable. A proportionality factor close to unity may suggest that the Raman scattering is highly correlated to the absorbance. Also, the value of the computed absorption coefficient is close to one of the vertical graphene sheets layers ($\sim 2x10^5 \text{cm}^{-1}$)[**?**] more than the one of PSi ($\sim 2x10^3 \text{cm}^{-1}$) or Si ($\sim 1.2x10^4 \text{cm}^{-1}$) at $\lambda = 532$nm[**?**]. This suggests that GPSi may have a high absorption coefficient, which could be true giving the fact of its marked dark aspect[**?**]. Moreover, we observe a saturation of the A_{D+G} ratio in Fig.2.B, that starts from a thickness of $\sim$ 250nm, which could also be seen as the maximum absorption depth for laser green wavelength in GPSi. This supports the fact that GPSi display a high absorption coefficient corresponding to $\sim 4x10^4 \text{cm}^{-1}$, approximately half of the computed value.

The set of conditions that were considered for an in-depth study of the nanocomposites are an O_2 plasma power of 20W and exposure time of 12s. It may be worth noting that a similar trend was seen for O_2-GPSi nanocomposite obtained on p-type Si (111) substrates compared to p-type Si (001) substrates (*see Fig. S3, supporting information file*).

We conduct a chemical etching tests with potassium hydroxide (KOH) solution to determine if the carbon remained within the bulk of the O_2-GPSi porous structure or not after O_2 plasma etching. The KOH solution considered in this study was an aqueous solution (30%), heated up at 40°C. The 125nm-thick mesoporous PSi, GPSi and O_2-GPSi samples were dipped in this solution for 2min. During the investigation, a considerable number of bubbles emerging from the PSi substrate was observed during KOH dipping. In case of O_2-GPSi, the KOH dipping showed more moderate degassing. This may suggest a faster etching rate for PSi compared to O_2-GPSi under heated KOH solution. Such a result was expected, considering that KOH solution is a well-known etching solution of Si[**?**], while the thin graphene-like coating seems to prevent the degradation of PSi structures in KOH solutions[**?**].

Figure 3: SEM micrographs of the cross sections and top views of 2min KOH dipped PSi (a and b), as-prepared GPSi (c and d) and 2min KOH dipped O_2-GPSi (e and f) substrates.

Fig. 3 illustrates the scanning electron microscopy (SEM) images of the porous nanocomposite morphology after the KOH treatment. The SEM images of PSi in Fig. 3(a-b), exhibit a sand dunes-like morphology with a complete etching of porous structure. Similar effect of KOH solution with various concentrations, on porous Si layers was previously reported by Matsuoka et al.[**?**]. In case of GPSi, the SEM images in Fig. 3(c-d), shows that the porous structure remained unchanged before and after KOH dip. On the other hand, the O_2-GPSi substrate display columnar morphology

(Fig. 3-e), comparable to the GPSi substrate before any O_2 plasma or KOH preparation steps. However, we can notice an increase of pore diameter at the surface of O_2-GPSi substrate after KOH dip (Fig. 3-f), which seem to roughly double in size. This may be explained by the O_2 plasma etching step that strips the surface from the graphene-like coating, which in return favors the surface dissolution by KOH. Moreover, the effect of thicker mesoporous PSi, GPSi and O2-GPSi structures (500nm thick) on KOH preparation was investigated and presented in *Fig. S4 of the supporting information file*, which reveals the passivation effect of the graphene-like coating on the pore's sidewall.

Fig. 4(a-c) depicts 5x5µm^2 AFM images of KOH dipped PSi, as-prepared GPSi and KOH dipped O_2-GPSi substrates. The dipped PSi substrate shows a high surface roughness with the root mean square (RMS) equal to 15.12nm (Fig. 4-a) due to a complete etching of the porous structure as it was exposed above by the SEM images of Fig. 3(a-b). On the other hand, a low RMS of 0.19nm was determined for as-prepared GPSi substrate (Fig. 4-b), while the dipped O_2-GPSi revealed an RMS=0.5nm (Fig. 4-c). The relative small difference in RMS values between as-prepared GPSi and O_2-GPSi substrates can be explained by the stripped surface of carbon. The Raman spectra of O_2-GPSi samples collected before and after KOH treatment (*see Fig. S5, supporting information file*), shows a minor change of A_{D+G} ratio. It may suggest that only a fraction of carbon near the top carbon-free surface of O_2-GPSi that was dissolved along with Si in KOH.

B. Growth of GaAs thin films

To confirm the validity of the surface preparation of the nanocomposite-based substrates for its intended application, epitaxial growth of GaAs layers has been carried out on the three 500nm-thick prepared substrates: PSi, GPSi and O_2-GPSi. Fig. 5(a) display the rocking curves of PSi, GPSi and O_2-GPSi substrates in the vicinity of the symmetrical GaAs (004) diffraction peak.

The X-ray rocking curves obtained on the GaAs/PSi heterostructure (top curve), display two peaks, one situated at 34.56°, corresponding to Si (004) peak of the substrate, and a second peak at 33.1°, attributed to the GaAs thin film with a full width at half maximum (FWHM) value of 406 arcsec[**?**]. However, on the GaAs/GPSi heterostructure (middle curve) the GaAs feature is almost imperceptible (*i.e.* very low peak intensity). A peak at 34.2° close to Si substrate peak is observed and can be assigned to the Si within the mesoporous layer that is strained by the presence of the

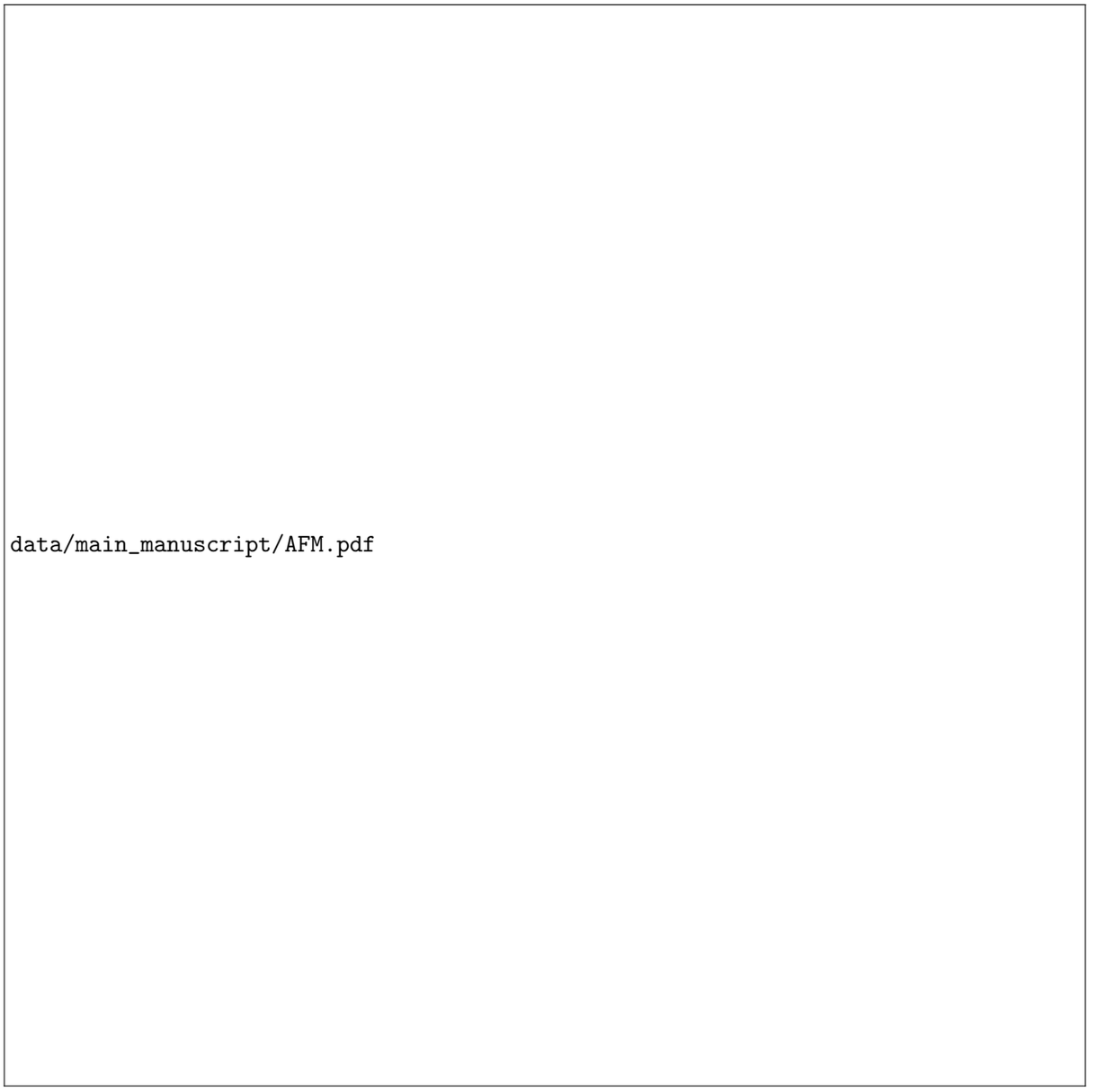

Figure 4: AFM images of 2min KOH dipped PSi (a), as-prepared GPSi (b) and 2min KOH dipped O_2-GPSi (c) substrates.

carbon coating[**?**]. The shift between the bulk Si and carbonized mesoporous Si peaks indicates a tensile strain caused by the carbonization process as determined by Boucherif et al.[**?**]. In the case of the GaAs/O_2-GPSi heterostructure (bottom curve), the XRD diffractogram reveals the presence of both Si and GaAs peaks. A FWHM value of 457 arcsec was measured for the GaAs peak indicating a crystalline quality equivalent to the one observed for GaAs/PSi heterostructure. The carbon-strained Si peak, present in the PSi sample is also present but weaker slightly shifted.

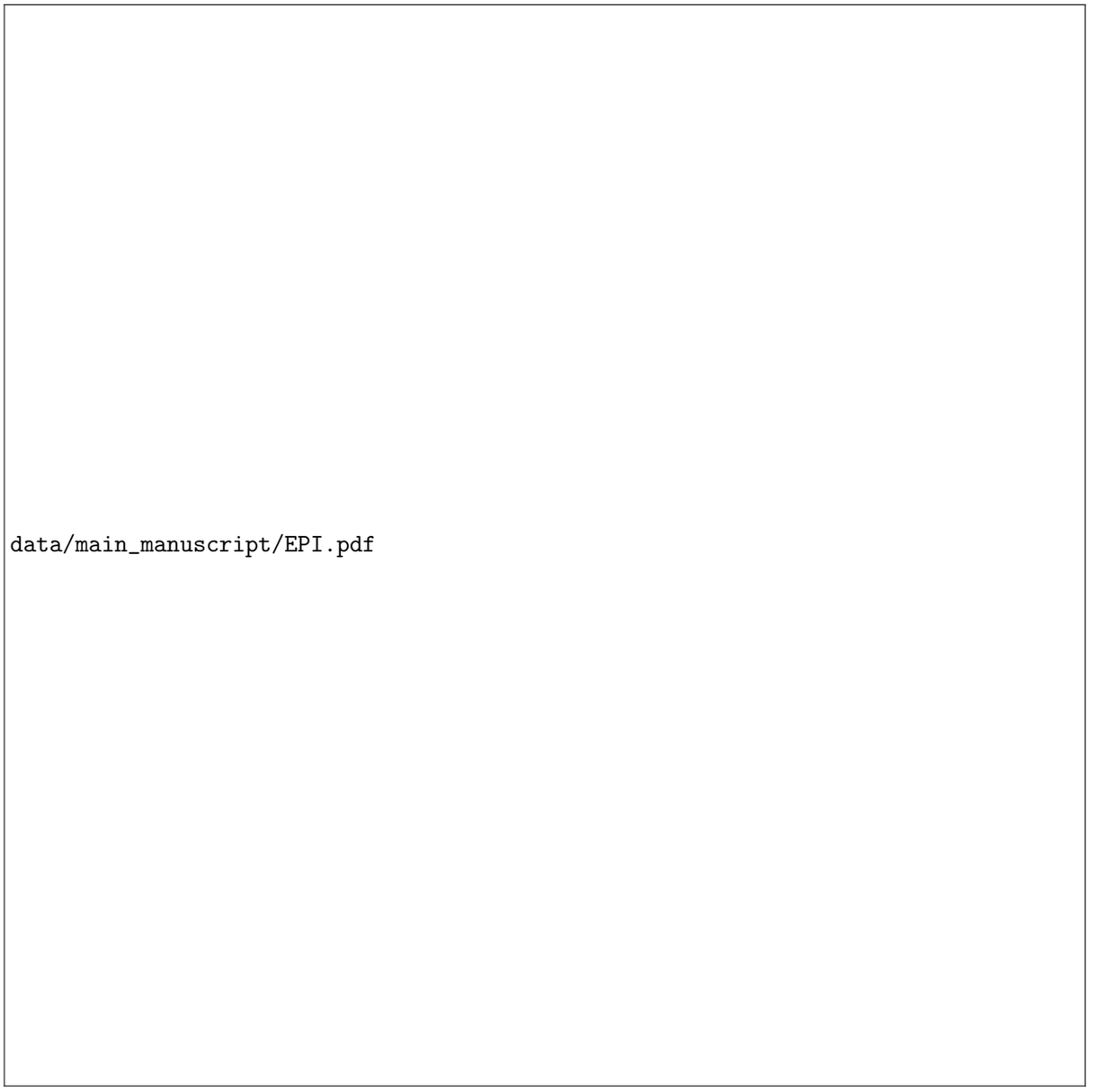

Figure 5: (a) X-ray diffractograms of epitaxial grown GaAs layer on PSi, GPSi and O_2-GPSi substrates and (b)-(d) cross-sectional SEM images showing GaAs morphology and mesoporous structure of the PSi, GPSi and O_2-GPSi substrates.

Such low intensity and position shift may be directly related to the carbon stripping of the top surface, but further work is needed to give a more definite conclusion.

Fig. 5(b-d) illustrates the cross-sectional SEM images which reveal the morphology of the GaAs layers grown on the PSi, GPSi, and O_2-GPSi substrates, respectively. The resulting GaAs morphology showed different lateral edge shapes on the three prepared mesoporous substrates.

The general morphology of the GaAs cleaved face for the GPSi suggests smaller grains or internal crystalline structures compared to the other two pictures. We interpret this as an indication of a polycrystalline or equivalent structure of the deposited GaAs for the GPSi only sample. This seems to be in agreement with the HR-XRD measurements and thus, confirming the effectiveness of O_2 plasma etching on striping the carbon from the GPSi surface, preparing it for epitaxial growth. Moreover, we can observe from cross-sectional SEM, a surface restructuration of the PSi mesoporous structure (bulk-like structure)[**?**]. In the case of GPSi and O_2-GPSi prepared substrates, no dense surface restructuration of the mesoporous structure can be observed.

The preservation of the mesoporous structure is associated with the presence of the graphene-like coating, which acts as a surface passivation agent that provides thermal stability to the mesoporous structure.

Consequently, the O_2-GPSi substrate seems attractive for epitaxial growth of materials with various lattice constants due to its thermally stable nanocomposite structure during epitaxial growth and due to its carbon-free top surface.

At this stage, we can conclude that a thermally stable nanocomposite structure, ready to accommodate the III-V heteroepitaxy was achieved with the use of O_2-GPSi substrate. However, we could not yet be able to appreciate the compliance of O2-GPSi over PSi, mainly because of the antiphase boundaries defects within GaAs epilayers which are inherent of this growth system[**?**]. The presence of these defects shade the potential benefits of using a thermally stable porous structure (O2-GPSi) instead of bulk-like one (PSi), as presume to give access to a suitable stress partition conditions during epitaxial growth.

IV. CONCLUSION

We have studied the preparation of a nanocomposite surface made of graphene-like coating and mesoporous silicon (GPSi) for subsequent epitaxial deposition. The GPSi surface was treated by oxygen plasma etching to obtain a carbon-free surface ready for epitaxial growth. The optimal conditions for O_2 plasma etching of the GPSi substrates were determined at a power of 20W and a total exposure time of 12s. With the given plasma etching conditions, the graphene-like coating is stripped efficiently from the nanocomposite top surface while remaining on the pore's sidewalls. The resulting substrate demonstrated thermal stability of the nanocomposite structure during GaAs epitaxial growth at a temperature of 565°C. In addition, the growth of GaAs thin

film on prepared nanocomposite has been demonstrated. At the same time, the mesoporous Si structure was preserved. This property makes it an attractive candidate as a compliant substrate for heteroepitaxial growth of various semiconductors thin films.

ACKNOWLEDGMENTS

The authors would like to thank G. Bertrand for technical help with epitaxy and carbonization process, H. Pelletier for technical help with epitaxy, P. Langlois for technical discussion about plasma process and to the Natural Sciences and Engineering Research Council of Canada (NSERC) and Fonds de Recherche du Quebec-Nature et Technologies (FRQNT) for financial support.

LN2 is a joint International Research Laboratory (Unité Mixte Internationale UMI 3463) funded and co-operated in Canada by Université de Sherbrooke (UdeS) and in France by CNRS as well as Université de Lyon (UdL, especially including ECL, INSA Lyon, CPE) and Université Grenoble Alpes (UGA). It is also associated to the French national nanofabrication network RENATECH and is supported by the Fonds de Recherche du Québec Nature et Technologie (FRQNT).

Journal of Vacuum Science Technology B

Journal of Vacuum Science Technology B

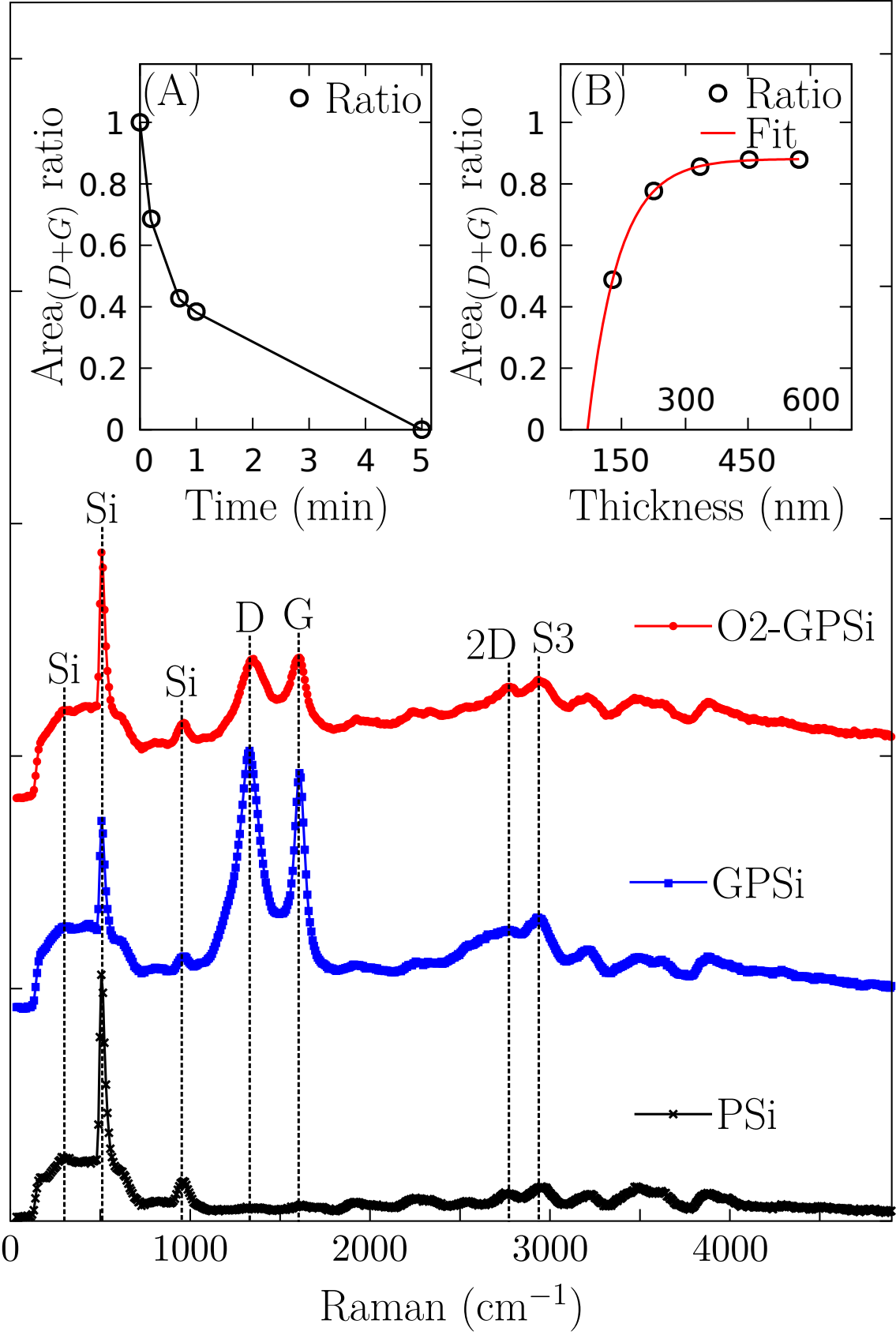

Journal of Vacuum Science Technology B

PLEASE CITE THIS ARTICLE AS DOI: 10.1116/6.0000423

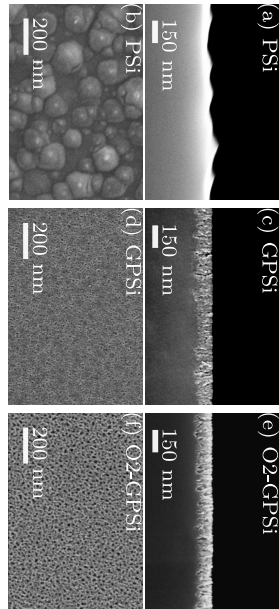

Journal of Vacuum Science Technology B

PLEASE CITE THIS ARTICLE AS DOI: 10.1116/6.0000423

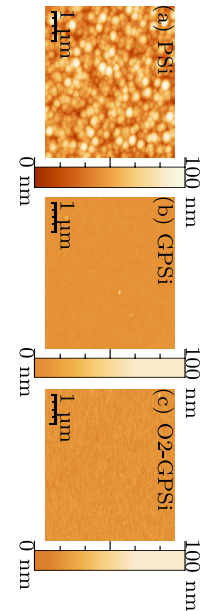

Journal of Vacuum Science Technology B

PLEASE CITE THIS ARTICLE AS DOI: 10.1116/6.0000423